ARTICLE

OBC
www.rsc.org/obc

Chiral receptors for phosphate ions

Valeria Amendola,[a] Massimo Boiocchi,[b] David Esteban-Gómez,[a] Luigi Fabbrizzi[a] and Enrico Monzani[a]

[a] *Dipartimento di Chimica Generale, Università di Pavia, via Taramelli 12, 27100, Pavia, Italy. E-mail: luigi.fabbrizzi@unipv.it; Fax: +39 0382 528544; Tel: +39 0382 987328*

[b] *Centro Grandi Strumenti, Università di Pavia, via Bassi 21, 27100, Pavia, Italy*

Received 7th April 2005, Accepted 18th May 2005
First published as an Advance Article on the web 16th June 2005

The binding tendencies of the enantiomeric forms, *R*,*R* and *S*,*S*, of the neutral receptor **1** towards anions were investigated through UV–vis and ^{1}H NMR titration experiments in DMSO. Both enantiomers form stable H-bond complexes with carboxylates and phosphates. In particular, receptor **1** strongly binds two $H_2PO_4^-$ ions according two stepwise equilibria, in which $\log K_2$ is higher than $\log K_1$. Such an unusual cooperativity effect is to be ascribed to the formation of strong H-bond interactions between the two $H_2PO_4^-$ anions, when bound to the two urea subunits of the receptor, as demonstrated by the crystal and molecular structures of the 1 : 2 complex salt: $[Bu_4N]_2[R,R\text{-}\mathbf{1}\cdots(H_2PO_4)_2]$. The *S*,*S* enantiomer forms an H-bond complex with the biologically relevant D-2,3-diphosphoglycerate anion, whose association constant is twice that of the *R*,*R* complex. Such an effect is ascribed to the different structural features of the two diastereomeric complexes in solution, as shown by ^{31}P NMR studies.

Introduction

There exists a current interest in the design of stereoselective receptors for neutral enantiomeric substrates, especially biologically important ones (*e.g.* amino acids, peptides).[1] However, much less attention has been paid to the study of abiotic selective receptors for chiral anions, which, nevertheless, play a prominent role in life.[2] A significant number of anion receptors operate as H-bond donors through the N–H fragment of amides,[3] ureas,[4] pyrroles.[5] Bonding selectivity essentially derives from multipoint interaction of the anion with the N–H groups placed in the hosting framework according to a favourable geometrical arrangement.[6–8] Enantiomeric selectivity can be induced by inserting a chiral fragment in a receptor's framework. As a common rule, the closer the chiral centre to the interaction site(s), the higher the enantiomeric discrimination exerted by the receptor.

In the purpose of designing a chiral anion receptor, we considered the 1,2-substituted cyclohexane subunit, which may exist in the two enantiomeric forms *R*,*R* and *S*,*S*. In particular, the *R*,*R*-cyclohexane-1,2-diamine subunit has been proven as a very useful compound in asymmetric synthesis,[9–12] and in enantiomeric and diastereoisomeric recognition of peptides.[13–19] The same fragment has been inserted into 22-membered hexamine macrocycles, which, in their protonated form, make enantioselective recognition of organic anions and *N*-protected amino acids.[20] In this study, two 4-nitrophenylurea subunits have been appended to the 1,2-cyclohexane moiety, to give **1**: 1-(4-nitrophenyl)-3-{2-[3-(4-nitrophenyl)ureido]cyclohexyl}urea.

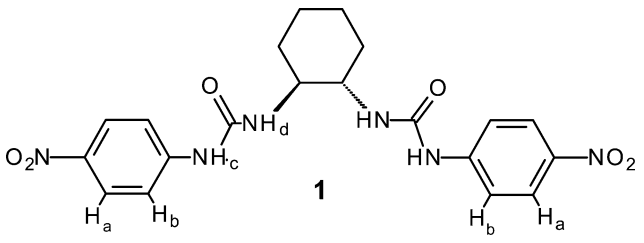

1

Urea is one of the most simple and classical neutral receptors for anions, being able to establish two directional H-bonds with Y-shaped anions like carboxylates.[21–27] The nitrophenyl group is expected to polarize the covalently linked urea N–H fragment, enhancing its H-bond donor properties. Moreover, the spectral features of the nitrobenzene chromophore can be altered by the interaction with the anion, thus providing a signal of the occurrence of the recognition process.[28] We report here on the interaction of **1**, both *R*,*R* and *S*,*S* enantiomers, in DMSO solution, with achiral oxoanions (acetate, benzoate, phosphate, pyrophosphate) and with the chiral and biologically relevant anion D-2,3-diphosphoglycerate.

Results and discussion

Achiral anions

A solution of *R*,*R*-**1** in DMSO (1.5×10^{-4}M) was titrated with a DMSO solution of $[Bu_4N]CH_3COO$, in a quartz cuvette, and thermostatted at 25 °C.

Fig. 1 displays the family of spectra obtained in the course of the titration. It is observed that the band centred at 350 nm (originating from a charge transfer transition from the closest N–H fragment to the $-NO_2$ group, across the phenyl ring) undergoes a moderate bathochromic shift on acetate addition. The presence of two isosbestic points, at 287 and 353 nm, indicates that only two species co-exist at the equilibrium. The titration profile (molar absorbance at 420 nm *vs.* equiv. of CH_3COO^-), shown in the inset of Fig. 1, suggests the formation of a 1 : 1 receptor–anion complex. Non-linear least-squares processing of titration data confirmed the occurrence of the equilibrium (eqn. (1)), whose $\log K$ value is 3.43 ± 0.03.

$$\mathbf{1} + CH_3COO^- \rightleftharpoons [\mathbf{1}\cdots CH_3COO]^- \quad (1)$$

More detailed pieces of information on the nature of the receptor–acetate interaction were obtained from ^{1}H NMR titration experiments.

Fig. 2 displays pertinent spectra obtained over the course of the titration of a 1.0×10^{-2} M solution of *R*,*R*-**1** in DMSO-d_6 with acetate. On anion addition, a pronounced downfield shift of all N–H protons was observed (limiting values $\delta(N\text{–}H_c) = 12.3$ ppm, $\delta/\text{ppm} = 3.0$; $\delta(N\text{–}H_d) = 9.0$ ppm, $\delta/\text{ppm} = 2.6$), which is indicative of the establishing of a genuine H-bond interaction. Moreover, a distinct downfield shift of the C–H_b protons is also observed ($\delta/\text{ppm} = 0.18$), whereas C–H_a protons are not affected by acetate addition. In this connection, it must be considered that hydrogen bond formation between the urea subunit and the anion can induce two distinct effects on the

DOI: 10.1039/b504931h

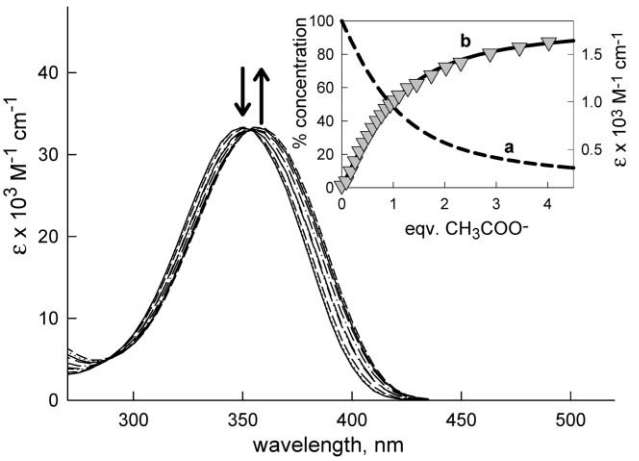

Fig. 1 Family of spectra taken in the course of the titration of DMSO 1.5×10^{-4} M in *R*,*R*-**1** with a standard solution of $[Bu_4N]CH_3COO$, at 25 °C. The titration profile in the inset, molar absorbance at 420 nm *vs.* equiv. of acetate, indicates the formation of a 1 : 1 adduct, $[\mathbf{1}\cdots CH_3COO]^-$, to which an association constant $\log K = 3.43 \pm 0.03$ corresponds (the profile refers to the titration performed on a 8.8×10^{-4} M solution of *R*,*R*-**1**). The distribution diagram of the species (% concentration, left side vertical axis) *vs.* equiv. of anion is also reported in the inset (% concentration of species: $\mathbf{a} = \mathbf{1}$, dashed line; $\mathbf{b} = [\mathbf{1}\cdots CH_3COO]$, solid line).

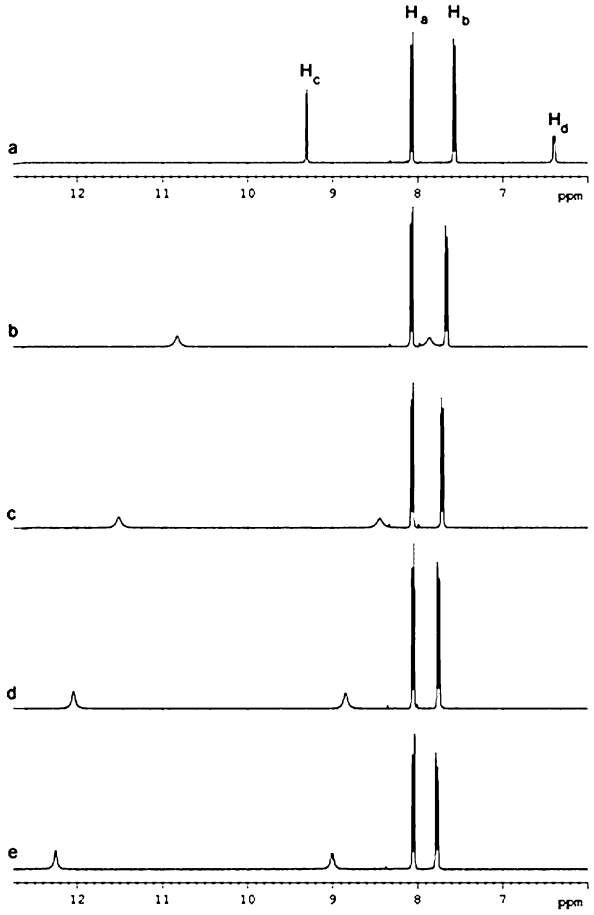

Fig. 2 Titration of a 10^{-2} M solution of *R*,*R*-**1** in DMSO-d_6 with CH_3COO^-. The reported spectra were registered after the addition of 0 equiv. (a), 0.3 equiv. (b), 0.6 equiv. (c), 0.9 equiv. (d) and 1.5 equiv. (e) of acetate.

aromatic substituents: (i) it increases the electron density in the phenyl rings, with a *through-bond* propagation: this causes a shielding effect and should induce an *upfield* shift of C–H protons; (ii) it promotes the polarisation of the C–H bonds, *via* a *through-space* effect: the partial positive charge created onto the proton causes a de-shielding effect and induces a *downfield* shift. The latter effect of electrostatic nature drastically decreases on increasing the distance from the site of H-bond interaction. The observed downfield shift of C–H_b protons indicates the predominance of the polarization effect. On the other hand, in the case of C–H_a protons, the polarization effect is smaller, in view of the larger distance from the N–H fragment, and is exactly compensated by the through-bond effect. Such an evidence would indicate the formation of a complex of the type whose structure is tentatively sketched in Scheme 1, in which the two oxygen atoms of the CH_3COO^- ion establish direct H-bond interactions with the four urea N–H groups of **1**. Notice that the 'flat' drawing of the $[R,R\text{-}\mathbf{1}\cdots CH_3COO]^-$ structural formula in Scheme 1 is a poor representation of the reality. In particular, due to the *trans* arrangement of the substituents of the 1,2-cyclohexane moiety, the two nitrophenyl–urea arms should lie on distinctly different planes.

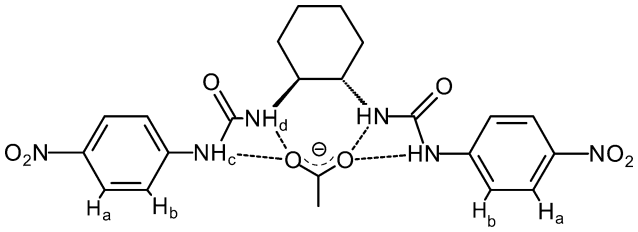

Scheme 1 Suggested structure of the $[R,R\text{-}\mathbf{1}\cdots CH_3COO]^-$ H-bond complex.

On non-linear least-squares fitting of $\delta(N\text{–}H_c)$ *vs.* CH_3COO^- equiv., a similar value of $\log K$ for the association equilibrium was calculated, which was affected by a larger standard deviation (3.4 ± 0.2).

Formation of a 1 : 1 complex was inferred from titration experiments with benzoate, for which a $\log K$ value of 2.86 ± 0.02 was determined. The lower stability of the $[R,R\text{-}\mathbf{1}\cdots C_6H_5COO]^-$ complex with respect to $[R,R\text{-}\mathbf{1}\cdots CH_3COO]^-$ can be ascribed to both the lower basicity of benzoate compared to acetate and steric repulsive interactions between the phenyl ring of the anion and the nitrophenyl substituents of the receptor.

Fig. 3 displays the UV–vis spectra recorded during the titration of DMSO solution of *R*,*R*-**1** with a standard solution of $[Bu_4N]H_2PO_4$, at 25 °C. On dihydrogenphosphate addition, a bathochromic shift of the charge transfer band at 350 nm is detected, more pronounced than that observed for CH_3COO^- (with $H_2PO_4^-$, $\lambda_{lim} = 370$ nm; with CH_3COO^-, $\lambda_{lim} = 366$ nm). Titration data are consistent with the occurrence of the two stepwise equilibria (2) and (3):

$$R,R\text{-}\mathbf{1} + H_2PO_4^- \rightleftharpoons [R,R\text{-}\mathbf{1}\cdots H_2PO_4]^- \quad (2)$$

$$[R,R\text{-}\mathbf{1}\cdots H_2PO_4]^- + H_2PO_4^- \rightleftharpoons [R,R\text{-}\mathbf{1}\cdots (H_2PO_4)_2]^{2-} \quad (3)$$

On non-linear least-squares processing of titration data, the following association constants were obtained: $\log K_1 = 2.96 \pm 0.02$ and $\log K_2 = 3.46 \pm 0.05$. It is suggested that the 1 : 1 complex possesses the same structure and tetrafurcate H-bonding arrangement hypothesized for acetate and sketched in Scheme 1. The lower stability of $[R,R\text{-}\mathbf{1}\cdots H_2PO_4]^-$ compared to $[R,R\text{-}\mathbf{1}\cdots CH_3COO]^-$ reflects the lower basicity and H-bond acceptor tendency of dihydrogenphosphate with respect to acetate. As regards the 1 : 2 complex $[R,R\text{-}\mathbf{1}\cdots (H_2PO_4)_2]^{2-}$, it is suggested that each $[H_2PO_4]^-$ ion interacts with one of the two urea subunits, giving bifurcate interaction. On this basis, one would expect that the second stepwise equilibrium, in which a tetrafurcate interaction is deleted and two bifurcated interactions are established, is substantially disfavoured with respect to the first one (neat formation of a tetrafurcate interaction). Thus, the unusual finding that $\log K_2$ is definitely higher than $\log K_1$ suggests the existence of a cooperativity effect,

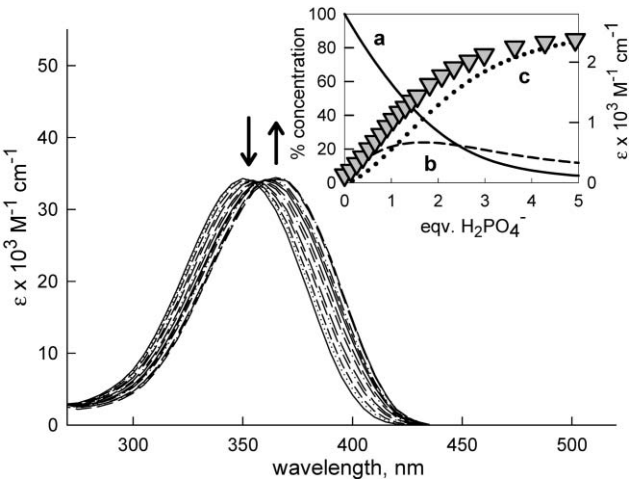

Fig. 3 Family of spectra taken in the course of the titration of DMSO solution 1.5×10^{-4} M in *R*,*R*-**1** with a standard solution of $[Bu_4N]H_2PO_4$, at 25 °C. The titration profile in the inset is consistent with the stepwise formation of the H-bond complexes $[R,R\text{-}\mathbf{1} \cdots H_2PO_4]^-$ and $[R,R\text{-}\mathbf{1} \cdots (H_2PO_4)_2]^{2-}$, to which the following association constants correspond: $\log K_1 = 2.96 \pm 0.02$ and $\log K_2 = 3.46 \pm 0.05$ (the profile of molar absorbance at 420 nm *vs.* equiv. of anion refers to the titration of a solution 9.5×10^{-4}M in *R*,*R*-**1**). The distribution diagram of the species (% concentration, left side vertical axis) *vs.* equiv. of anion is also reported in the inset (% concentration of species: **a** = *R*,*R*-**1**, solid line; **b** = $[R,R\text{-}\mathbf{1} \cdots H_2PO_4]^-$, dashed line; **c** = $[R,R\text{-}\mathbf{1} \cdots (H_2PO_4)_2]^{2-}$, dotted line).

whose nature can be hardly inferred from spectroscopic titration data.

A good chance to clarify the nature of the $R,R\text{-}\mathbf{1} \cdots H_2PO_4$ interactions has been provided by crystallisation of colourless crystals of a salt of formula $[Bu_4N]_2[R,R\text{-}\mathbf{1}\cdot(H_2PO_4)_2\cdot[CH_3CN]$, obtained from an MeCN solution containing *R*,*R*-**1** and an excess of $[Bu_4N]H_2PO_4$, saturated with diethylether. Crystal size was suitable for single crystal X-ray diffraction analysis and the crystallographic study was performed.

The crystal structure is characterized by infinite dihydrogenphosphate chains along the *a* axis, similar with those observed for alkylammonium salts of $H_2PO_4^-$. [29,30,31] In particular, each $H_2PO_4^-$ ion interacts with two adjacent $H_2PO_4^-$ groups and one *R*,*R*-**1** receptor *via* H-bonds (see Fig. 4).

In solution, dihydrogenphosphate oligomers are probably absent and the bis-urea receptor binds a hydrogen bonded dihydrogenphospate dimer, forming the $[R,R\text{-}\mathbf{1} \cdots (H_2PO_4)_2]^{2-}$ anion shown in the ORTEP diagram in Fig. 5. It can be observed that each $H_2PO_4^-$ ion establishes two H-bond interaction with one of the two urea subunits of the receptor. Moreover, the two dihydrogenphosphate anions interact with each other through two O–H $\cdots$ O bonds, each anion behaving as both an H-bond donor and an H-bond acceptor. It is therefore suggested that the energy contribution from this inter-anionic interaction is responsible for the extra-stability of the $[R,R\text{-}\mathbf{1} \cdots (H_2PO_4)_2]^{2-}$ complex in solution, thus accounting for the observed cooperativity effect ($\log K_2 > \log K_1$). Notice that such an interanionic interaction cannot by established by the CH_3COO^- ion, which, in fact, does not form any 1 : 2 complex with *R*,*R*-**1**. Features of the X–H $\cdots$ O interactions (X = O, N) in the crystalline complex are reported in Table 1.

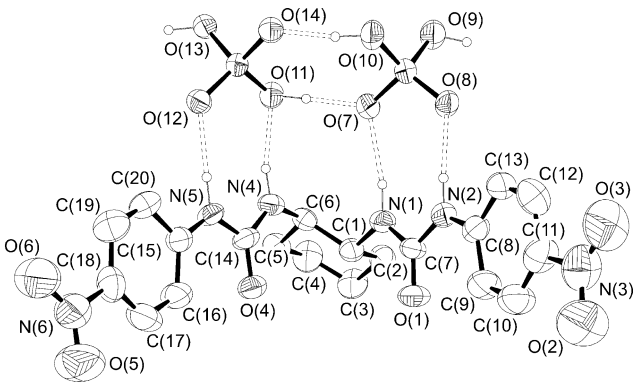

Fig. 5 An ORTEP view of the anionic H-bond complex $[R,R\text{-}\mathbf{1} \cdots [H_2PO_4]_2]^{2-}$ (thermal ellipsoid are drawn at the 30% probability level, only H atoms involved in intermolecular hydrogen bonds are drawn, two $[Bu_4N]^+$ ions and a CH_3CN solvent molecule have been omitted for clarity). Dashed lines indicate the hydrogen bond interactions in the asymmetric unit.

Formation of H-bond complexes in DMSO solution is confirmed by ^{1}H NMR titration experiments: Fig. 6 shows representative spectra taken in the course of the titration. The downfield shift of N–H protons indicates the occurrence of an H-bond interaction with the anion (limiting values $\delta(N\text{–}H_c) = 11.8$ ppm, $\delta/\text{ppm} = 2.5$; $\delta(N\text{–}H_d) = 9.0$ ppm, $\delta/\text{ppm} = 1.5$).

The pattern is similar to that observed in the case of acetate, but the limiting values reached by the N–H urea protons are noticeably lower, as expected in view of the lower basicity and

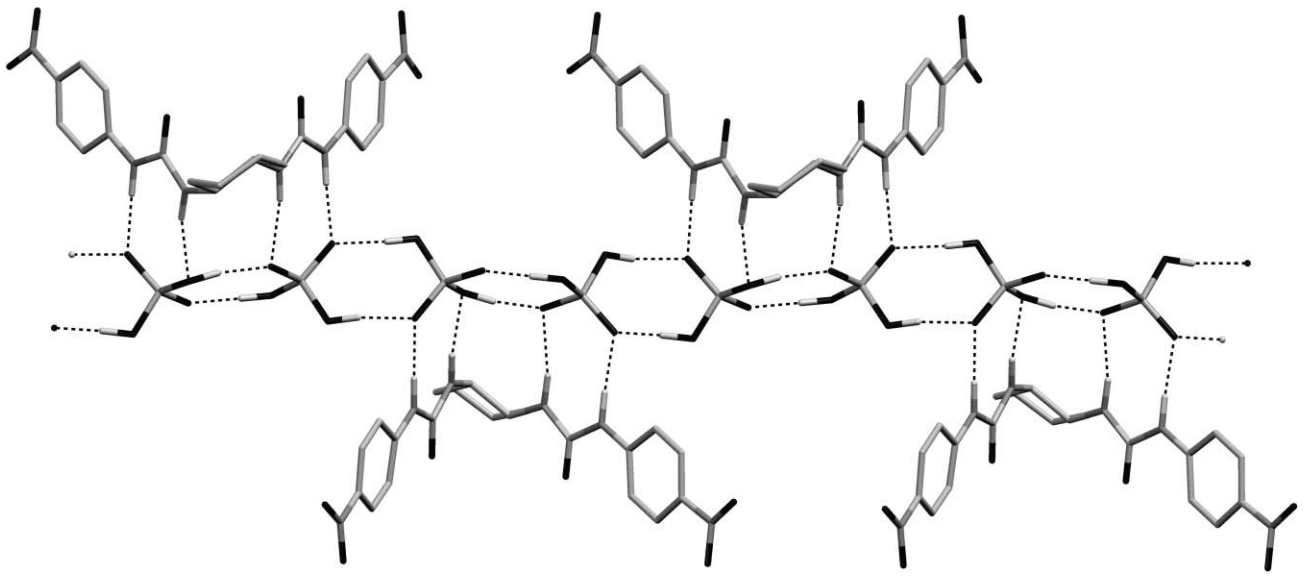

Fig. 4 A simplified sketch showing the $[H_2PO_4]^-$ chain along the *a* axis and the H-bond motif of the $[Bu_4N]_2[R,R\text{-}\mathbf{1}\cdot(H_2PO_4)_2]$ crystal. $[Bu_4N]^+$ ions have been omitted for clarity.

Table 1 Features of the H-bond interactions in the $[R,R\text{-}\mathbf{1}\cdots[H_2PO_4]_2]^{2-}$ complex (X = N, O)

Donor group	D···A/Å	H···O/Å	X–H···O/°	Acceptor atom
N(1)–H(1N)	3.03(1)	2.19(1)	166.3(6)	O7
N(2)–H(2N)	2.84(1)	1.98(1)	174.4(5)	O8
N(4)–H(4N)	2.87(1)	2.06(1)	156.6(6)	O11
N(5)–H(5N)	2.85(1)	1.99(1)	179.4(5)	O12
O(10)–H(10O)	2.52(1)	1.62(3)	159.0(24)	O14
O(11)–H(11O)	2.53(1)	1.63(3)	156.6(31)	O7
O(9)–H(9O)	2.64(1)	1.72(5)	163.4(45)	O(12)[a]
O(13)–H(13O)	2.59(1)	1.79(5)	140.0(23)	O(8)[b]

Symmetry code:[a] $= x + 1/2, -y + 1/2, -z + 2$; [b] $= x - 1/2, -y + 1/2, -z + 2$

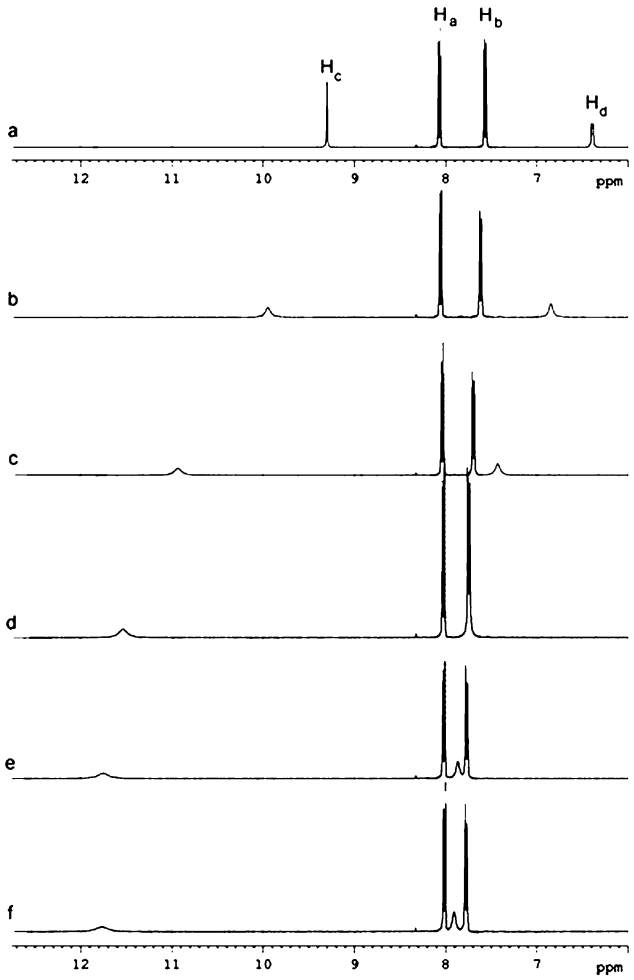

Fig. 6 Titration of a 1.0×10^{-2} M solution of *R,R*-**1** in DMSO-d_6 with $[H_2PO_4]^-$. The reported spectra were registered after the addition of 0 equiv. (a), 0.4 equiv. (b), 1.2 equiv. (c), 1.8 equiv. (d), 2.7 equiv. (e), 4.2 equiv. (f) of $[H_2PO_4]^-$.

H-bond acceptor tendency of dihydrogenphosphate. Moreover, it has to be noted that, in the 1 : 2 adduct with $H_2PO_4^-$, the negative charge of each anion is not only addressed to the H-bond with the receptor, but also to the interaction with the other bound dihydrogenphosphate ion, as shown in the X-ray structure. Due to the polarization effect, C–H_b protons undergo a downfield shift to the same extent as observed in the titration with acetate (δ/ppm = 0.18). On the other hand, a slight but definite upfield shift of C–H protons is observed. This indicates the occurrence of a through-bond propagation of negative charge on the phenyl ring. Notice that, in spite of the different H-bonding arrangement, differentiating the spectroscopic behaviour of the 1 : 1 and 1 : 2 complexes is not straightforward and no clear discontinuity is observed on moving from the first to the second added equiv. of dihydrogenphosphate. This is due to the fact that $\log K_2 > \log K_1$, which makes the $[R,R\text{-}\mathbf{1}\cdots(H_2PO_4)_2]^{2-}$ complex form early in the titration (well before 1 equiv. addition), and coexist with the $[R,R\text{-}\mathbf{1}\cdots(H_2PO_4)]^-$ species (indeed, this is clearly shown in the concentration distribution diagram in the inset of Fig. 3). Due to the relatively high concentration of the receptor (67-fold higher than in spectrophotometric titration experiments), plots of δ(N–H_c) and δ(N–H_d) *vs.* $H_2PO_4^-$ equiv. showed steep saturation profiles, which prevented from a safe determination of association constants.

The affinity of receptor *R,R*-**1** towards a pair of phosphate ions prompted us to the investigation of its interaction with pyrophosphate. Fig. 7 shows the family of UV–vis spectra taken over the course of the titration of a DMSO solution of *R,R*-**1** (5.4×10^{-4}M) with $[Bu_4N]_3HP_2O_7$, at 25 °C.

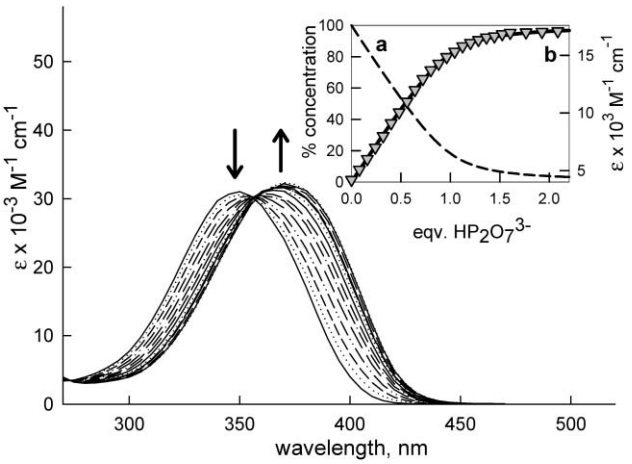

Fig. 7 Family of spectra taken over the course of the titration of DMSO solution 5.4×10^{-4}M in *R,R*-**1** with a standard solution of $[Bu_4N]_3HP_2O_7$, at 25 °C. The titration profile in the inset indicates the formation of the 1 : 1 H-bond complex $[R,R\text{-}\mathbf{1}\cdots HP_2O_7]^{3-}$, to which the following association constant corresponds: $\log K = 4.63 \pm 0.03$. The distribution diagram of the species (% concentration, left side vertical axis) *vs.* equiv. of anion is superimposed (% concentration of species: **a** = *R,R*-**1**, dashed line; **b** = $[R,R\text{-}\mathbf{1}\cdots HP_2O_7]^{3-}$, solid line).

The titration profile, shown in the inset of Fig. 7, clearly indicates the formation of a stable 1 : 1 H-bond complex, for which an association constant $\log K = 4.63 \pm 0.03$ was calculated.

On ^{1}H NMR titration with $HP_2O_7^{3-}$ of a 10^{-2} M solution of *R,R*-**1** in DMSO-d_6 with, at 25 °C, broad and poorly resolved signals were obtained, which indicates the formation of a rather rigid complex. On increasing temperature to 70 °C, a clearer pattern was obtained, which is shown in Fig. 8.

On hydrogenpyrophosphate addition, signals of N–H protons disappeared, probably due to temperature enhanced proton exchange. Then, downfield shift of C–H_b protons and upfield shift of C–H_a protons were observed, the effects being more pronounced than for the formation of the $[(R,R)\text{-}\mathbf{1}\cdots(H_2PO_4)]^-$ complex. This suggests the establishment of stronger H-bond interaction, which may be due both to an especially favourable geometrical complementarity between the receptor and the

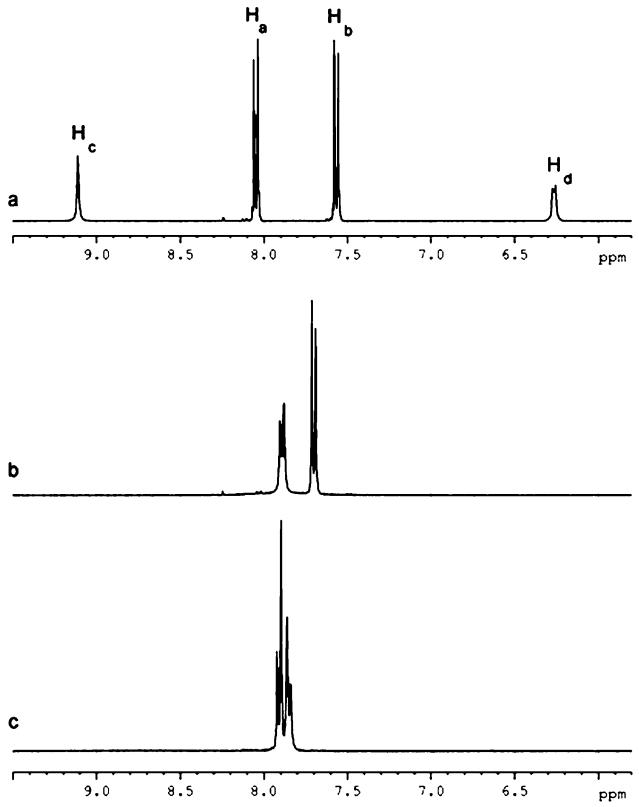

Fig. 8 Spectra recorded over the course of the titration of a 1.0×10^{-2} M solution of *R*,*R*-**1** in DMSO-d_6 with $HP_2O_7^{3-}$, at 70 °C. The reported spectra were registered after the addition of 0 equiv. (a), 0.5 equiv. (b), 1.0 equiv. (c) of $HP_2O_7^{3-}$.

anionic substrate and to the higher negative charge detained by $HP_2O_7^{3-}$, with respect to the two $H_2PO_4^-$ ions.

The same spectrophotometric titration experiments were carried out on the *S*,*S*-**1** receptor. Values of the association constants of the complexes formed with CH_3COO^-, $C_6H_5COO^-$, $H_2PO_4^-$, $HP_2O_7^{3-}$, obtained through non-linear least-squares treatment of titration data, are reported in Table 2. Values are coincident with those obtained for the *R*,*R*-**1** receptor, as expected in view of the achiral nature of the investigated anions.

Chiral anions: D-2,3-diphosphoglycerate

Differences in recognition properties of *R*,*R*-**1** and *S*,*S*-**1** enantiomers should be detected in presence of a chiral anion. Thus, in view of the observed affinity of **1** towards diphosphates, we considered the biologically relevant D-2,3-diphosphoglycerate anion, **2**, which contains two $-OPO_3^{3-}$ groups and one $-COO^-$. **2** is a glycolytic intermediate, resulting from the interconversion between D-1,3-diphosphoglycerate and D-3-phosphoglycerate catalyzed by phosphoglycerate mutase.[32] Moreover, **2** is an allosteric effector, which regulates the oxygenation level of haemoglobin. As a matter of fact, in physiological conditions, the D-2,3-diphosphoglycerate is present in human erythrocytes at approximately the same concentration as haemoglobin and regulates the oxygen binding activity of the protein, by binding preferentially to its deoxygenated form.[33–35] A metal containing achiral synthetic receptor for 2,3-diphosphoglycerate, displaying a high selectivity in water, has been recently reported.[36] Such a receptor is capable of depriving haemoglobin of 2,3-diphosphoglycerate, thus indirectly controlling the oxygenation level of the protein.

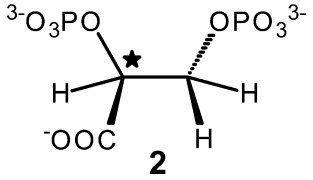

2

The problem we faced first in this study was the low solubility of the sodium salts of **2** in DMSO and other commonly used organic aprotic solvents. Attempts to prepare tetraalkylammonium salts failed, giving in any case unrecoverable oils. Fortunately, the cyclohexylammonium salt of **2** ($[RNH_3]_5X$) is commercially available, displaying an acceptable solubility in DMSO (up to 3×10^{-4}M). Then, a DMSO solution of $[RNH_3]_5X$ (10^{-4}M) was titrated with a standard DMSO solution of **1**, either *R*,*R* or *S*,*S*. The absorbance data (at the wavelengths for which the molar absorbance of the adduct was higher than the molar absorbance of **1**, *i.e.* from 418 to 430 nm) were plotted against the receptor equivalents, as shown in Fig. 9.

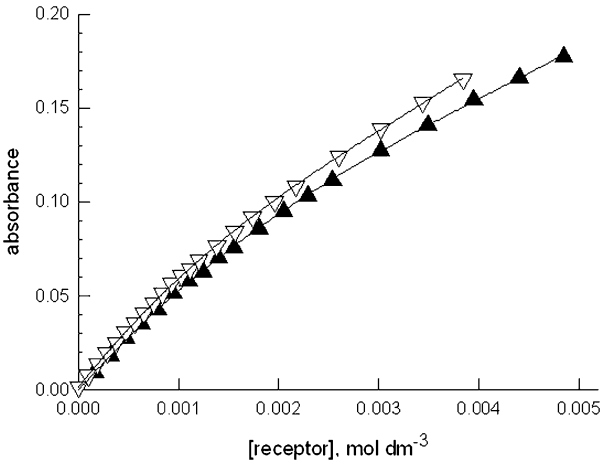

Fig. 9 Plots of absorbance at 415 nm *vs.* molar concentration of receptor (*S*,*S*-**1**, open symbols; *R*,*R*-**1**, filled symbols). The titrations were performed under identical conditions, by adding aliquots of a standard solution of **1** (0.05 M, in DMSO) to a 3×10^{-4}M solution of **2** in DMSO (path length: 0.1 cm). Solid lines were obtained through non-linear least-squares treatment of titration data.

For both *R*,*R*-**1** and *S*,*S*-**1**, a smooth curvature of the plot was observed. However, the steeper curvature of the pertinent plot (▽ symbols in Fig. 9) clearly indicated that the *S*,*S* receptor forms a more stable complex with X^- than the *R*,*R* analogue (▲ symbols). On non-linear least-squares fitting of the two plots the following log*K* values for the formation of the 1 : 1 complex were calculated: *R*,*R*-**1**, 2.52 ± 0.02; *S*,*S*-**1**, 2.87 ± 0.05. The low values of the stability constants compared to those determined for pyrophosphate could be explained as a result of steric

Table 2 Log*K* values for the interaction equilibria of the two enantiomers *R*,*R*-**1** and *S*,*S*-**1** with achiral anions in DMSO at 25 °C, spectrophotometrically determined. Values in parentheses correspond to the standard deviation on the last significant figure

Anion	Equilibrium	*R*,*R*-**1**	*S*,*S*-**1**
CH_3COO^-	$\mathbf{1} + CH_3COO^- \rightleftharpoons [\mathbf{1} \cdots CH_3COO]^-$	3.38(3)	3.37(5)
$C_6H_5COO^-$	$\mathbf{1} + C_6H_5COO^- \rightleftharpoons [\mathbf{1} \cdots C_6H_5COO]^-$	2.86(2)	2.89(3)
$H_2PO_4^-$	$\mathbf{1} + H_2PO_4^- \rightleftharpoons [\mathbf{1} \cdots H_2PO_4]^-$	2.96(2)	2.93(5)
	$[\mathbf{1} \cdots H_2PO_4]^- + H_2PO_4^- \rightleftharpoons [\mathbf{1} \cdots (H_2PO_4)_2]^{2-}$	3.46(5)	3.40(9)
$HP_2O_7^{3-}$	$\mathbf{1} + HP_2O_7^{3-} \rightleftharpoons [\mathbf{1} \cdots HP_2O_7]^{3-}$	4.63(3)	4.66(3)

and electrostatic repulsive effects. In particular, the distance between the phosphate groups in the 2,3-diphosphoglycerate anion is considerably larger than in pyrophosphate, which may force the receptor to deviate from its relaxed and energetically favored conformation. Furthermore, the cyclohexylammonium counterions might compete in solution with the receptor for the anion, thus reducing the value of the association constants. In any case, the neat difference of 0.35 between the measured log$K$ values is well beyond the values of standard deviations and expresses the differential affinity, of chiral origin, of *S*,*S*-**1** towards D-2,3-diphosphoglycerate, with respect to *R*,*R*-**1**.

Then, ^{1}H NMR and ^{31}P NMR studies were carried out, in order to obtain structural details on the two diastereomeric complexes in solution. In particular, in each experiment, an excess of **2** (7 : 1 molar ratio) was added as a solid to a 10^{-2} M suspension of 1 in DMSO-d_6, either *R*,*R* or *S*,*S* enantiomer. The obtained mixture was sonicated and filtered (in order to enhance solubility, spectra were all registered at 70 °C); then, the concentration of **2** compared to **1** could be determined from the integral ratio in the ^{1}H NMR spectrum. With both *R*,*R*-**1** and *S*,*S*-**1**, the calculated amount of **2** in solution was below the equivalence, due to the low solubility of the anion in DMSO. As an interesting result, a different solubility of **2** was observed in the presence of the two enantiomeric hosts. In particular, in presence of *R*,*R*-1, the concentration of the anion was 60% of that of the receptor, and 80% in presence of *S*,*S*-**1**. The different solubility of **2** in the presence of the receptor confirms the different stability of the diastereomeric complexes.

In Fig. 10, the ^{1}H NMR signals of *R*,*R*-**1** and *S*,*S*-**1** are reported. Spectral differences (spectrum a: *R*,*R* complex; b: *S*,*S* complex) mainly refer to the chemical shifts of N–H protons, as directly involved in the H-bond. In particular, N–H protons

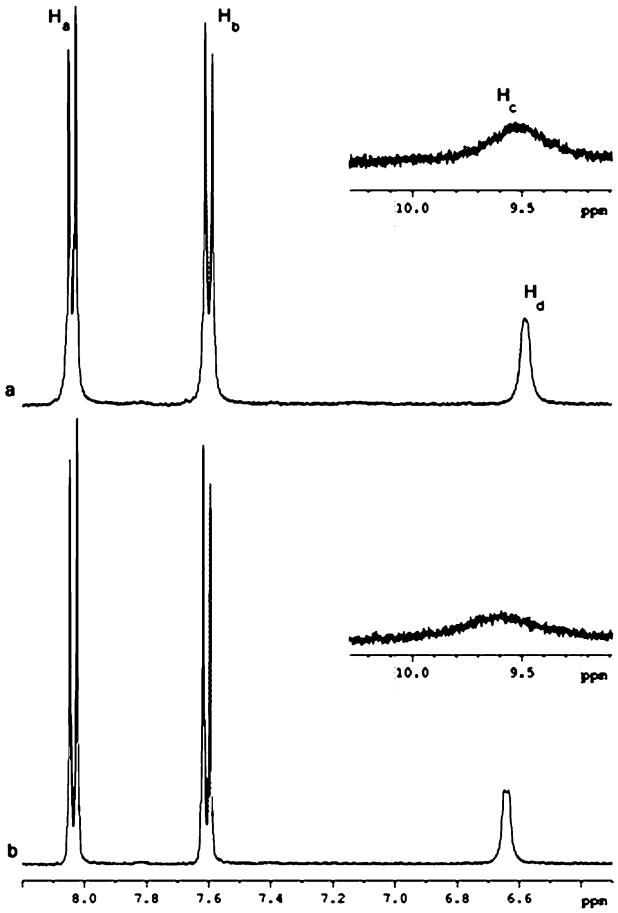

Fig. 10 ^{1}H NMR spectra recorded at 70 °C on a 10^{-2}M solution of *R*,*R*-**1** (spectrum a) and *S*,*S*-**1** (spectrum b), in the presence of **2** in DMSO-d_6. In the reported range of ppm, only the signals of **1** are shown.

are more downfield shifted in the presence of *S*,*S*-**1** (limiting value δ(N–H$_c$) = 9.6 ppm; δ/ppm = 0.5, compared to the uncomplexed receptor) than in the presence of *R*,*R*-1 (δ(N–H$_c$) = 9.5 ppm; δ/ppm = 0.4). This behaviour can be associated to the larger amount in solution of the complexed *S*,*S* receptor. Useful pieces of information were obtained from the ^{1}H NMR and ^{31}P NMR spectra of anion **2** (Fig. 11 and 12, respectively). Since the concentration of **2** was lower than that of **1**, the anion in solution could be considered as completely bound to the receptor.

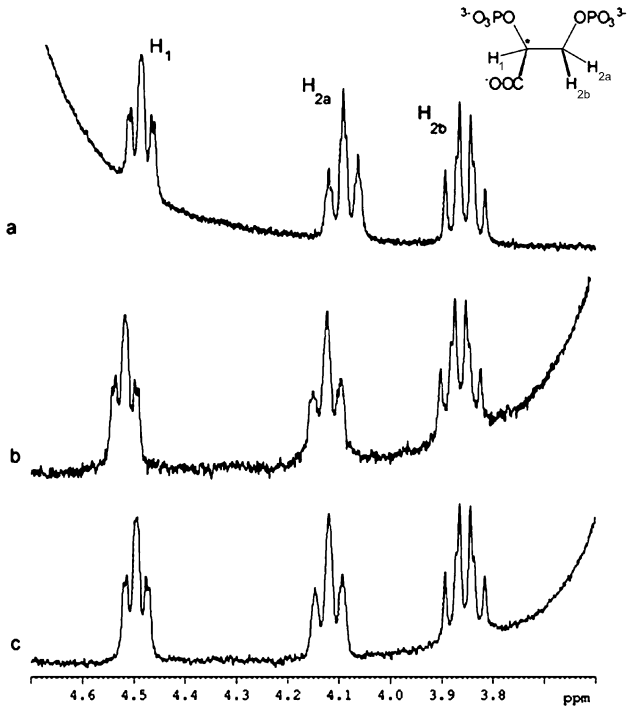

Fig. 11 ^{1}H NMR spectra recorded in DMSO-d_6 at 70 °C, on a solution of D-2,3-diphosphoglycerate alone (spectrum a); in the presence of (*R*,*R*)-**1** (b); in the presence of (*S*,*S*)-**1** (c).

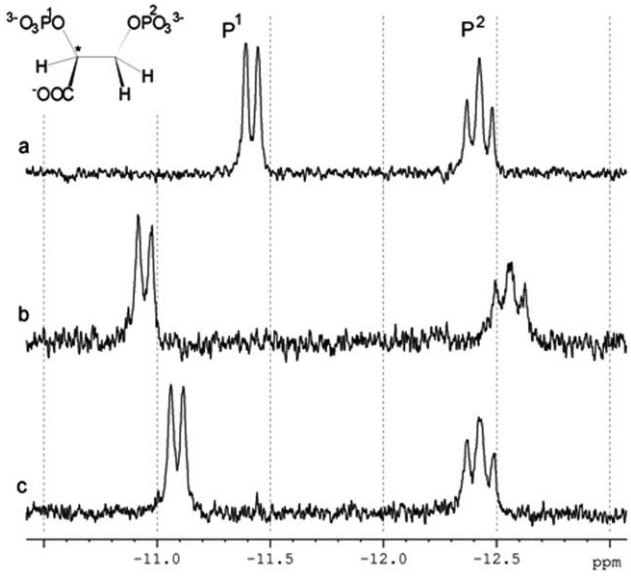

Fig. 12 ^{31}P NMR spectra recorded in DMSO-d_6 at 70 °C, on a solution of D-2,3-diphosphoglycerate: alone (spectrum a); in the presence of *R*,*R*-**1** (b); in the presence of *S*,*S*-**1** (c).

As regards ^{1}H NMR spectra (Fig. 11), the main difference between the two complexes is observed in the chemical shift of proton H$_1$ (compare spectra b and c). Notice that H$_1$ belongs to the chiral centre and must be particularly sensitive

to the diastereotopic environment of the complex. In the ^{31}P NMR spectra too, the difference between the complexes relies mostly on the phosphorus bound to the chiral center (P_1 in Fig. 12). In particular, it is observed that, in both ^1H NMR and ^{31}P NMR spectra, the *R*,*R*-**1** complex shows larger shifts of the D-2,3-diphosphoglycerate signals than the *S*,*S*-**1** analogue. This could be attributed to the fact that, in complex formation, the *R*,*R* receptor undergoes a more endoergonic conformational rearrangement, which is consistent with the lower value of the association constant. It has also to be noticed that complexation induced only little variations on the chemical shifts of the D-2,3-diphosphoglycerate protons. Actually, these protons are too far from the sites of interaction with the receptor and are principally influenced by the structural rearrangement of **2**, which accompanies the complexation. In conclusion, NMR studies indicated that the two diastereomeric complexes, characterized by different stability constants, possess distinctly different structures in solution. In particular, the ^1H and ^{31}P NMR spectra showed that significant, and presumably endoergonic, rearrangements of both receptor and anion take place in the formation of the less stable complex, $[R,R\text{-}\mathbf{1}\cdots X]^{5-}$.

Conclusion

The effect of the chiral *trans*-1,2-cyclohexane subunit on the enantiselective recognition of anions by neutral receptors has been investigated. In particular, on appending two urea containing arms to either the *R*,*R* or *S*,*S* enantiomeric form of *trans*-1,2-cyclohexane, two chiral receptors for difunctional anions were obtained. Enantioselective tendencies of *R*,*R* and *S*,*S* receptors were tested toward the biologically relevant chiral anion D-2,3-diphosphoglycerate. This may appear as a counterintuitive approach, since the usual procedure consists of designing one given chiral receptor and testing its recognition properties on pairs of enantiomeric substrates. In any case, this study has demonstrated that a chiral discriminating effect exists, even if not spectacular, for the envisaged receptors, which corresponds to a difference of 0.35 log units in binding constants (and of 2.0 kJ mol^{-1} in binding energies). It has to be noted that previously investigated cyclic polyammonium receptors, incorporating one or two *trans*-cyclohexane subunits, were able to discriminate pairs of enantiomeric anions with $\Delta\log K$ varying from 0.1 to 0.6 (for 1 : 1 complexes).[20] Chiral selectivity has an essentially steric nature and affects only indirectly the main receptor–substrate interaction. Such a steric influence increases on decreasing the distance between steric interaction sites and in particular that between the chiral centres in host and guest. Moreover, chiral selectivity is expected to increase on increasing the rigidity of receptor's framework and introducing steric constraints onto it. In this sense, receptor **1** could be considered a convenient base for the development of efficient neutral enantioselective receptors for chiral anions.

Experimental

General procedures and materials

All reagents for syntheses were purchased from Aldrich/Fluka and used without further purification. UV–Vis spectra were recorded on a Varian CARY 100 spectrophotometer, with a quartz cuvette (path length: 1 or 0.1 cm). The cell holder was thermostatted at 25.0 °C, through circulating water. ^1H NMR spectra were obtained on a Bruker AVANCE400 spectrometer (400 MHz), operating at 9.37 T. Spectrophotometric titrations were performed on 10^{-4}–10^{-3} M solutions of **1** in DMSO (polarographic grade). Typically, aliquots of a fresh alkyl-ammonium salt standard solution of the envisaged anion (CH_3COO^-, $C_6H_5COO^-$, $H_2PO_4^-$, $HP_2O_7^{3-}$) were added to the solution of **1**, whose UV–vis spectra were recorded. Because of the low solubility of the alkyl-ammonium D-2,3-diphosphonate-butyrate salt in DMSO, the titration were performed by adding aliquots of a standard solution of **1** in DMSO to a 10^{-4} M solution of the anion in the same solvent. All spectrophotometric titration curves were fitted with the HYPERQUAD program.[37] Care was taken that in each titration the *p* parameter (p = [concentration of complex]/[maximum possible concentration of complex]) was lower than 0.8, a condition required for the safe determination of a reliable equilibrium constant.[38] ^1H NMR titrations were carried out on DMSO-d_6 solutions, at 10^{-3}–10^{-2} M concentration of the receptor. ^{31}P NMR spectra were carried out on DMSO-d_6 solutions containing $[Bu_4N]PF_6$ as an internal reference.

Synthesis of 1,1-(4-nitrophenyl)-3-{2-[3-(4-nitrophenyl)ureido]cyclohexyl}urea (1)

4-Nitrophenylisocyanate (0.64 g, 3.90 mmol) was added to a solution of *R*,*R*-cyclohexane-1,2-diamine (0.022 g, 1.63 mmol) in $CHCl_3$ (50 mL), in a round flask filled with argon. The mixture was refluxed under magnetic stirring for 4 h, then was left stirring at room temperature for further 12 h. During the reaction, the yellow 4-nitrophenylisocyanate slowly dissolved and a white precipitate formed. The product was collected by filtration, washed with water (3 × 7 mL) and dried *in vacuo* (0.57 g; yield: 80%). $C_{20}H_{22}N_6O_6$ (442.4 g mol^{-1}). ^1H NMR (DMSO-d_6, δ_H/ppm): $\delta = 9.3$ (1H, s, NH_c), 8.1 (2H, d, CH_a), 7.6 (2H, d, CH_b), 6.4 (1H, d, NH_d), 3.5 (1H, br s, –CH_2CH_2CH–N), 2.0 and 1.8 (2H, 2 br s, –CH_2CH_2CHN), 1.5 (2H, br s, –CH_2CH_2CHN). IR (nujol mull), cm^{-1}: 1741 (C=O); 1577 ν(N–O); 1461 $\nu_{as}(NO_2)$; 1301 $\nu_s(NO_2)$; 3365, 3339 ν_{as}, ν_s(N–H), 1498, 1249 δ_{as}, δ_s(N–H). The synthesis of the *S*,*S* receptor was performed as described for the *R*,*R* enantiomer. In particular, from 0.64 g of 4-nitrophenylisocyanate (3.90 mmol) and 0.022 g of *S*,*S*-cyclohexane-1,2-diamine (0.163 mmol), 0.54 g of white and pure product were obtained (yield: 75%). The ^1H NMR (in DMSO-d_6) and the IR spectra were identical to the ones recorded for *R*,*R*.

X-Ray crystallographic studies†

Diffraction data were collected at room temperature by means of an Enraf-Nonius CAD4 four circle diffractometer, working with graphite-monochromatized Mo Kα X-radiation ($\lambda = 0.71073$ Å). Crystal data for the $[Bu_4N]_2[R,R\text{-}\mathbf{1}\cdot(H_2PO_4)_2\cdot[CH_3CN]$ salt: $C_{54}H_{101}N_9O_{14}P_2$; M 1162.38; pale yellow colour; orthorhombic, $P2_12_12_1$ (no. 19); a 17.059(3) Å, b 19.498(5) Å, c 19.657(3) Å, V 6538(2) $Å^3$; Z 4; ρ_{calcd} 1.181 g cm^{-3}; μ Mo $K\alpha$ 0.131 mm^{-1}; 8008 measured reflections, 7590 unique reflections (R_{int} 0.0456), 3662 strong reflections [$I_O > 2\sigma(I_O)$]; $R1$ and w$R2$ (strong data) 0.0771 and 0.1864; $R1$ and w$R2$ (all data) 0.1662 and 0.2367. Flack parameter 0.17(26). Data reductions (including intensity integration, background, Lorentz, and polarization corrections) were performed with the WinGX package.[39] Absorption effects were evaluated with the ψ-scan method,[40] and absorption correction was applied to the data (0.919 and 0.943 min and max transmission factor). The crystal structure was solved by direct methods (SIR 97)[41] and refined by full-matrix least-squares procedures on F^2 using all reflections (SHELXL 97).[42] Anisotropic displacement parameters were refined for all nonhydrogen atoms. Hydrogens belonging to the organic moieties were placed at calculated positions with the appropriate AFIX instructions and refined using a riding model. Hydrogens of the H_2PO_4 groups were located in the ΔF map and their position refined with soft geometrical restraints on the O–H distance and on the P–O–H angle.

† CCDC reference numbers 268368. See http://www.rsc.org/suppdata/ob/b5/b504931h/ for crystallographic data in CIF or other electronic format.

Acknowledgements

The financial support of the European Union (RTN Contract HPRN-CT-2000-00029) and of the Italian Ministry of University and Research (PRIN-Dispositivi Supramolecolari; FIRB-Project RBNE019H9K) is gratefully acknowledged.

References

1 A. P. Davis, Chiral Guest Recognition, in *Encyclopedia of Supramolecular Chemistry*, ed. J. L. Atwood, J. W. Steed, Marcel Dekker, New York, 2004, pp. 236–244.
2 R. J. Fitzmaurice, G. M. Kyne, D. Douheret and J. D. Kilburn, *J. Chem. Soc., Perkin Trans. 1*, 2002, 841–864.
3 S. Valiyaveetil, J. F. J. Engbersen, W. Verboom and D. N. Reinhoudt, *Angew. Chem., Int. Ed. Engl.*, 1993, **32**, 900–901.
4 P. J. Smith, M. V. Reddington and C. S. Wilcox, *Tetrahedron Lett.*, 1992, **41**, 6085.
5 J. L. Sessler, M. J. Cyr, V. Lynch, E. McGhee and J. A. Ibers, *J. Am. Chem. Soc.*, 1990, **112**, 2810–2813.
6 *Supramolecular Chemistry of Anions*, ed. A. Bianchi, K. Bowman-James and E. García-España, Wiley-VCH, New York, 1997.
7 P. D. Beer and P. A. Gale, *Angew. Chem., Int. Ed.*, 2001, **40**, 486–516.
8 *Coord. Chem. Rev.*, 2003, **240**, 1-226. Special Issue: 35 Years of Synthetic Anion Receptor Chemistry 1968-2003, ed. P. A. Gale.
9 B. M. Trost and R. C. Bunt, *Angew. Chem., Int. Ed. Engl.*, 1996, **35**, 99.
10 B. M. Trost, R. Radinov and E. M. Grenzer, *J. Am. Chem. Soc.*, 1997, **119**, 7879.
11 M. Palucki, N. S. Finney, P. J. Pospisil, M. L. Gler, T. Ishida and E. N. Jacobsen, *J. Am. Chem. Soc.*, 1998, **120**, 948.
12 S. E. Schaus, J. Branalt and E. N. Jacobsen, *J. Org. Chem.*, 1998, **63**, 403.
13 N. Farrell, D. M. Kiley, W. Schmidt and M. P. Hacker, *Inorg. Chem.*, 1990, **29**, 397.
14 K. Skog and O. Wennerström, *Tetrahedron Lett.*, 1992, **33**, 1751.
15 S. S. Yoon and W. C. Still, *J. Am. Chem. Soc.*, 1993, **115**, 823.
16 W. C. Still, *Acc. Chem. Res.*, 1996, **29**, 155.
17 J. Reedijk, *Chem. Commun.*, 1996, 801.
18 Z. Pan and W. C. Still, *Tetrahedron Lett.*, 1996, **37**, 8699.
19 F. Gasparrini, D. Misiti, W. C. Still, C. Villani and H. Wennemers, *J. Org. Chem.*, 1997, **62**, 8221.
20 I. Alfonso, B. Dietrich, F. Rebolledo, V. Gotor and J.-M. Lehn, *Helv. Chim. Acta.*, 2001, **84**, 280–295.
21 E. Fan, S. A. van Arman, S. Kincaid and A. D. Hamilton, *J. Am. Chem. Soc.*, 1993, **115**, 369–370.
22 J. Scheerder, J. F. J. Engbersen, A. Casnati, R. Ungaro and D. N. Reinhoudt, *J. Org. Chem.*, 1995, **60**, 6448–6454.
23 M. P. Hughes, M. Shang and B. D. Smith, *J. Org. Chem.*, 1996, **61**, 4510–4511.
24 M. P. Hughes and B. D. Smith, *J. Org. Chem.*, 1997, **62**, 4492–4499.
25 A. J. Evans, S. E. Matthews, A. R. Cowley and P. D. Beer, *Dalton Trans.*, 2003, 4644–4650.
26 H. Miyaji, S. R. Collinson, I. Prokes and J. H. R. Tucker, *Chem.Commun.*, 2003, 64–65.
27 M. Barboiu, G. Vaughan and A. van der Lee, *Org. Lett.*, 2003, **5**, 3074–3076.
28 M. Boiocchi, D. Esteban-Gómez, L. Fabbrizzi, M. Licchelli and E. Monzani, *J. Am. Chem. Soc.*, 2004, **124**, 16507–16514.
29 J. M. Karle and I. L. Karle, *Acta Crystallogr., Sect. C: Cryst. Struct. Commun.*, 1988, **44**, 1605.
30 N. Ohama, M. Machida, T. Nakamura and Y. Kunifuji, *Acta Crystallogr., Sect. C: Cryst. Struct. Commun.*, 1987, **43**, 962.
31 M. E. Light, S. Camiolo, P. A. Gale and M. B. Hursthouse, *Acta Crystallogr., Sect. E Struct. Rep. Online*, 2001, **57**, 727.
32 S. I. Winn, H. C. Watson, R. N. Harkins and L. A. Fothergill, *Philos. Trans. R.. Soc. London, Ser. B.*, 1981, **293**, 121–130.
33 R. Benesch and R. E. Benesch, *Nature*, 1969, **221**, 618–621.
34 A. Arnone, *Nature*, 1972, **237**, 146–149.
35 R. Benesch, R. E. Benesch and C. I. Yu, *Proc. Natl. Acad. Sci. USA*, 1968, **59**, 526–532.
36 Z. Zhong and E. V. Anslyn, *Angew. Chem., Int. Ed.*, 2003, **42**, 3005–3008.
37 P. Gans, A. Sabatini and A. Vacca, *Talanta*, 1996, **43**, 1739–1753.
38 C. S. Wilcox, in *Frontiers in Supramolecular Chemistry and Photochemistry*, ed. H.-J. Schneider and H. Dürr, Wiley-VCH, Weinheim, 1991, pp. 123-143.
39 L. J. Farrugia, *J. Appl. Crystallogr.*, 1999, **32**, 837–838.
40 A. C. T. North, D. C. Phillips and F. S. Mathews, *Acta Crystallogr., Sect. A: Cryst. Phys., Diffr., Theor. Gen. Cryst.*, 1968, **24**, 351–359.
41 A. Altomare, M. C. Burla, M. Camalli, G. L. Cascarano, C. Giacovazzo, A. Guagliardi, A. G. G. Moliterni, G. Polidori and R. Spagna, *J. Appl. Crystallogr.*, 1999, **32**, 115–119.
42 G. M. Sheldrick, *SHELX97: Programs for Crystal Structure Analysis*; University of Göttingen, Göttingen, Germany, 1997.